SITE AND SOURCE EFFECTS IDENTIFIED FROM TWO-PEAK RESPONSE SPECTRA (2PRS)

G.R. Saragoni[(1)], M.F. Gallegos [(2)]

[(1)] *Principal Professor, Department of Civil Engineering, Universidad de Chile, rsaragon@ing.uchile.cl*

[(2)] *Ph.D. Student, Department of Structural and Geotechnical Engineering, Pontificia Universidad Catolica de Chile, mfgallegos@uc.cl*

Abstract

Two-peak response spectra (2PRS) have often been observed in epicentral or near-field accelerograms recorded in soft soils after the occurrence of subduction earthquakes during the last 35 years. One of the peaks represents the highest energy content of the earthquake (short periods) while the other one the dynamic response of the soil (sites with a long predominant period). Usually, the soil peak is similar or larger amplitude than the source peak. This unique feature is associated with the separated participation effect of the source from the soil response in different stages of energy release from the dominating asperities of the subducted plate. However, recent evidence depicts that this type of spectra could be also observed for earthquakes in other non-subduction zones.

In this work, 2PRS corresponding to accelerograms registered in soft soils for the latest subduction and non-subduction earthquakes are investigated. The studied seismic events produced significant economic impacts, building collapses and consequently losses of lives in the last decade: Chile, 2010; New Zealand 2011; Japan, 2011; Nepal, 2015; Ecuador, 2016; Italy 2016; and Mexico, 2017. The outcomes reveal that the period of soil peak has a good correlation with both the one estimated by the Nakamura method and the other from low energy pulses detected in spectrograms. In addition, for earthquakes related to short faults of a few kilometers, the amplitude of the soil peak never surpasses the first peak.

The actual importance of 2PRS for earthquake engineering is that source peak affects houses or middle-rise buildings, and soil peak affects high-rise or base-isolated buildings, both effects in the same seismic event. Therefore, design response spectra considered in national seismic codes for soft soils should be modified in the future in order to consider both effects.

Keywords: site effect; seismic source; two-peak response spectra; earthquakes; accelerograms.

1. Introduction

Accelerograms of large subduction earthquakes have a long duration of some minutes due to their fault rupture length of hundreds of kilometers. These long durations are in contrast with the short duration of ten seconds of most crustal earthquakes related to fault length of few ten kilometers. In the first instance, the difference leads that in long-duration accelerograms of mega earthquakes is possible to observe in response spectra the separated participation effect of the source from the soil response in different stages of the energy release from the dominating asperities of the subducted plate [1]. This attribute of subduction accelerograms registered in epicentral or near-field sites leads to absolute response spectra with two separated peaks for source and soft soil effects [2].

Saragoni et al. [3] reported two-peak ground-motion response spectra (2PRS) for the first time after analyzing acceleration time histories of the M 7.8 Central Chile earthquake that occurred in 1985. The authors found 2PRS in Viña del Mar station (near the epicenter) for both horizontal components. Later, motivated by the low representativeness of response spectra achieved as a result of averaging accelerograms, Lobos [4] studied the accelerograms of the 1985 Central Chile earthquake, and Gómez [5] studied the accelerograms obtained for 1985 Mexico earthquake recorded in the Mexico City basin. Both authors proposed the need to develop response spectra with more than one peak representing the periods observed in the studied accelerograms.

Chile, unlike other countries, has registered some accelerograms of mega-earthquakes in epicentral locations over the years. This fact has allowed studying the seismic behavior of soils in conditions close to the design cases. Analyzing these accelerograms, Saragoni & Ruiz [6] identified the presence of two characteristic peaks in Chilean earthquakes, concluding that one is due to seismic source and another due to soil period. Afterward, Ruiz & Saragoni [7] proposed absolute acceleration design spectra for the “NCh 433 Of. 96” Chilean seismic code considering two peaks as a consequence of the soil effect and the type of earthquake, being pioneers in this type of initiative. Later, Ruiz & Saragoni [8] found 2PRS, using the accelerograms from epicentral areas of large magnitude earthquakes close to the design magnitude, avoiding mixing with small amplitude accelerograms corresponding to earthquakes of small and moderate magnitudes. This regard was considered because the energy in seismic source periods was observed exclusively in epicentral accelerograms of large earthquakes. The main conclusion was that the proposed design 2PRS contemplated the Nazca plate subduction, but it might be expanded to other subduction or non-subduction zones. Finally, Idini et al. [9] developed new ground-motion prediction equations (GMPE) for subduction zones to be used in modern seismic hazard analysis. The authors could predict two-peak ground-motion response spectra for interface and intraslab earthquakes at soil sites with a long predominant period.

Summing up the literature, 2PRS were often detected in epicentral accelerograms recorded in soft soils after the occurrence of subduction earthquakes in Mexico and Chile. The first peak in short periods is due to the source effect, and the second peak in longer periods is due to soil response effect. Usually, the soil peak is similar or larger amplitude than the source peak.

However, recent evidence depicts that this type of spectra could also be observed for earthquakes in other non-subduction zones. The purpose of this study is to investigate 2PRS corresponding to accelerograms registered in soft soils for recent earthquakes. The selected earthquakes produced significant structural and non-structural damages of buildings and consequently losses of lives in the last decade: M 8.8 El Maule, Chile (2010); M 6.1 Christchurch, New Zealand (2011); M 9.1 Tohoku, Japan (2011); M 7.8 Gorkha, Nepal (2015); M 7.8 Muisne, Ecuador (2016); M 6.2 Norcia, Italy (2016); and M 7.1 Puebla - Morelos, Mexico (2017). In addition, natural periods are estimated for the relating soil deposits applying both the Nakamura method and spectrogram technique, demonstrating that the peak in longer periods is always related to the soil deposit response.

2. Analysis of recent earthquakes

2.1 El Maule, Chile earthquake (2010):

On February 27, a magnitude M 8.8 earthquake struck the south-central part of Chile. The rupture occurred in the contact between the Nazca and the South American plates, with an approximate extension of 500 km in the north-south direction. As the rupture spread, the fault slip generated earthquake shaking and warped the ocean floor, triggering a tsunami along the fault-rupture area [10].

Free vibration of soils frequently occurs during some large earthquakes, perhaps seeming like a paradox. This fact could be due to the energy released from seismic sources, especially of their asperities, is not stationary in time, allowing relaxation intervals in between without important seismic wave arrivals in which free vibration of soil happens [11]. The occurrence of El Maule earthquake offered a great opportunity to validate those assumptions. The natural period of free vibrations from acceleration time histories of the 2010 event was estimated by Saragoni & Ruiz [1], applying two techniques: autocorrelograms and Fourier spectra. The observed free vibrations of soil satisfied the one-dimension elastic S-wave propagation theory, where the free vibration modal periods obeyed the natural period equation (Eq. (1)).

$$Tn = \frac{4\,H}{Vs\,(2\,n - 1)} \tag{1}$$

where Tn = natural period; H = soil depth; Vs = soil shear wave velocity; and n = mode number.

The research findings are illustrated in Figures 1 and 2. Fig.1a depicts the longitudinal component of the accelerogram recorded in the Concepcion Centro station, where free vibrations are indicated. A comparison of displacements calculated by integrating twice the accelerograms for the records of Concepción Centro and Concepción San Pedro stations is shown in Fig.1b. The free vibrations of soil were observed in the displacement time history of the Concepcion Centro station, in the interval of relaxation without the arrival of important seismic waves that occur between the arrival of two seismic pulses 1 (t_1=13 sec) and 2 (t_2=29 sec). Pulses are similar in both stations (related with two main asperities of Nazca plate), confirming that these were due to the seismic source. Field soil studies suggest that the natural period of soil in downtown Concepcion is 2.1 seconds, whereby Fig.1b presents a lower number of cycles for Concepcion Centro station in the relaxation interval, concerning the number of cycles for San Pedro station.

Fig.2a illustrates absolute acceleration response spectra for 5% critical damping, corresponding to Concepción Centro accelerograms. When the soil response is deterministically dominated in most of the accelerograms, response spectra are characterized to have a single peak, as indicated by most seismic design codes. However, when the accelerations are recorded at epicentral areas specifically in soft soils, the response spectra are more complex, presenting two clear peaks such as Concepcion Centro response spectra (for both horizontal components). The spectrum for longitudinal component presents one peak around 2.1 seconds, which would belong to the free vibrations of soft soil; and another peak between 0.3 and 0.7 seconds, due to probably the interaction of the waves associated with the seismic source and the response of higher ground modes (second and third vibration modes).

Fig.2b presents the acceleration time history for the Concepcion Centro station for the longitudinal component. Free vibrations of 2.1 seconds (0.5 Hz) for this accelerogram can be seen in the time interval of relaxation between 16 – 27 seconds in the spectrogram of Fig.2c. This period would coincide with a depth to bedrock of 120 m and a shear wave velocity of 250 m/s for the sandy soil of Concepcion [1] using Eq. (1). The great relevance of the Concepcion accelerogram is due to this record was obtained few blocks from where a 15-story reinforced concrete building collapsed. The iconic "Alto Rio" building collapsed in the first 20 seconds during the source effect without soil response influence [12], showing the importance of 2PRS in the current seismic design.

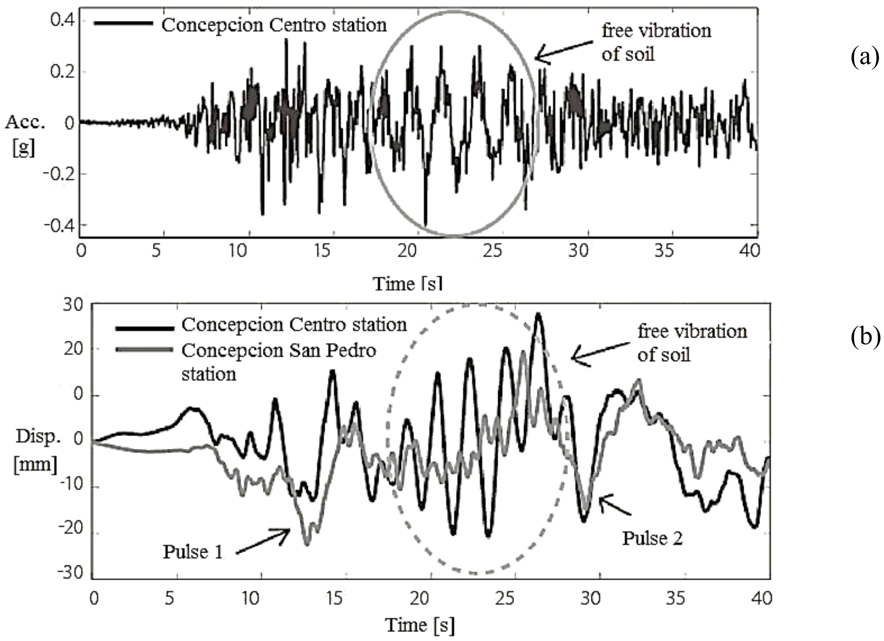

Fig. 1 – 2010 Chile earthquake: (a) Accelerogram of Concepcion Centro station with free harmonic vibration of soil. (b) Comparison of ground displacements of Concepcion Centro and San Pedro stations, indicating similar seismic pulses. (modified from [1]).

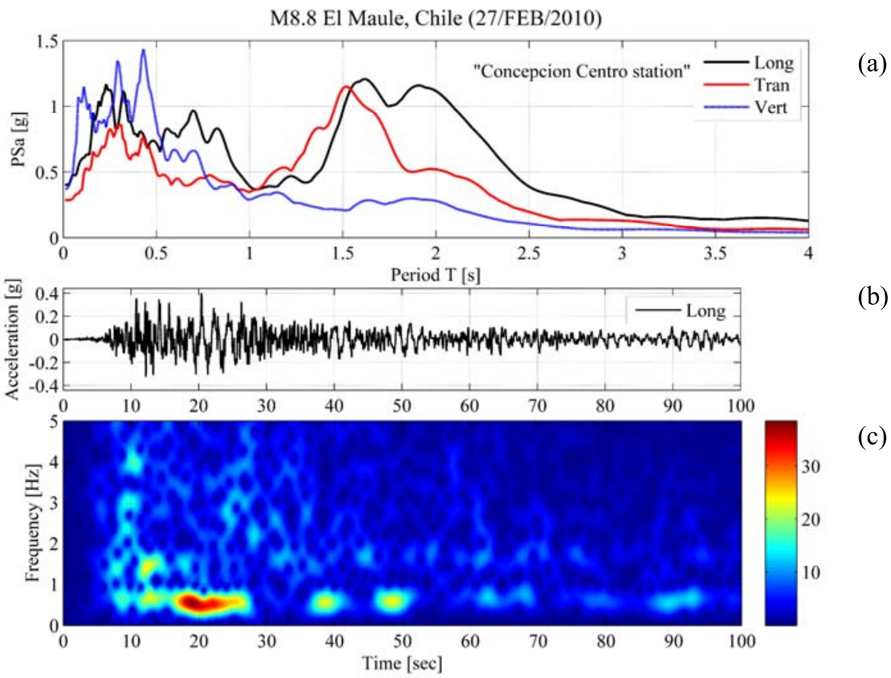

Fig. 2 – 2010 Chile earthquake recorded at Concepcion Centro station: (a) 5%-damped acceleration response spectra (2PRS). (b) Acceleration time history for the longitudinal component. (c) Spectrogram for the longitudinal component. (after [1]).

2.2 Christchurch, New Zealand earthquake (2011)

The February 21, M 6.1 earthquake occurred as part of the aftershock sequence of the M 7.0 September 3, 2010 Darfield, NZ earthquake. This earthquake involved oblique-thrust faulting at the easternmost limit of previous aftershocks, and like the mainshock itself is broadly associated with regional plate boundary deformation as the Pacific and Australia plates interact in the central South Island, New Zealand [13]. The aftershock occurred on an unmapped fault less than 8 km from the Christchurch city center resulting in the collapse of two reinforced concrete office buildings and one concrete parking garage, and severe damage to numerous others.

One unique aspect of this earthquake was the very high vertical ground accelerations, frequently exceeding the peak horizontal accelerations at recording station within approximately 10 km of the epicenter. Fig.3a shows 5%-damped acceleration response spectra for the Christchurch Cathedral College station. Both horizontal acceleration responses show two peaks at periods of 0.6 and 1.3 seconds, respectively. Fig.3b presents the acceleration time history for this station for the N64E component, and the spectrogram of Fig.3c depicts low energy pulses of 1.3 second (0.7 Hz).

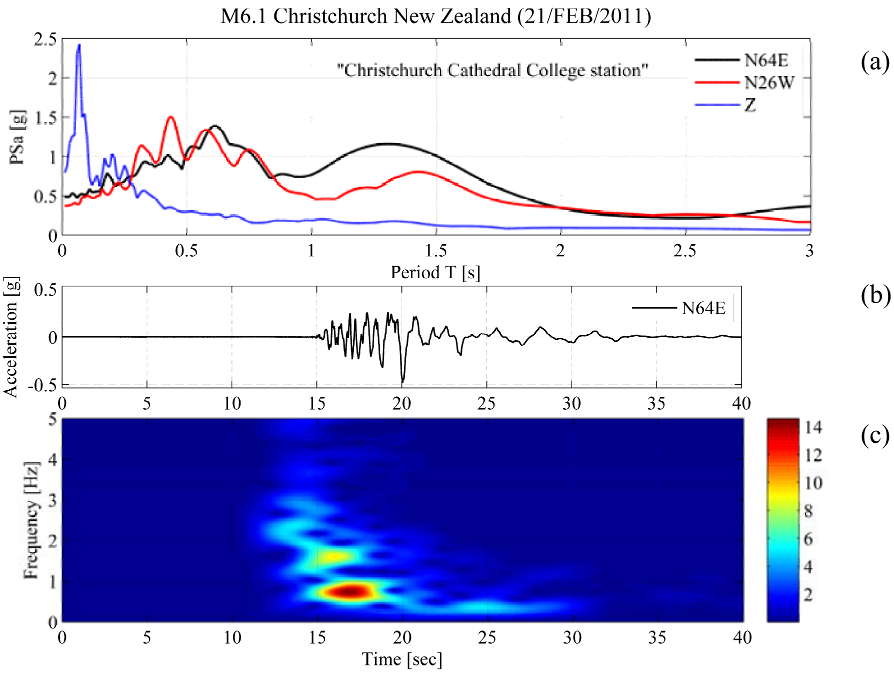

Fig. 3 – 2011 Japan earthquake recorded at MYG013 station: (a) 5%-damped acceleration response spectra (2PRS). (b) Acceleration time history for the N-S component. (c) Spectrogram for the N-S component.

2.3 Tohoku, Japan earthquake (2011)

The March 11, M 9.1 Tohoku earthquake, which occurred near the northeast coast of Honshu, Japan, resulted from shallow thrust faulting on the subduction zone plate boundary between the Pacific and North America plates. At the location of this earthquake, the Pacific plate moves roughly westward relative to the North America plate at a velocity of 83 mm/yr and begins its westward descent beneath Japan at the Japan Trench, east of the March 11th earthquake. The location, depth (about 25 km) is consistent with the event having occurred on the subduction zone plate boundary, and the fault slipped over an area approximately 400 km long (along strike) by 150 km wide (in the down-dip direction) [10].

Strong motion records at over 30 stations in Miyagi Prefecture from this earthquake were obtained by various organizations, including the Japan Meteorology Agency (JMA). Fig.4a shows 5%-damped acceleration response spectra for MYG013 station, which has high acceleration responses in a range of periods (T=0.2 and 0.7-1.0 seconds). Fig.4b presents the acceleration time history for this station for the N-S component. Two energy releases at 50 and 90 seconds are appreciated, probably related to both dominant asperities of the subducted plate. At 80 seconds, a free vibration of the soil deposit could be estimated in the spectrogram of Fig.4c at a 1.0 second (1.0 Hz).

Although the Tohoku region (in the North-Eastern part of Japan) was hard hit this time, Japan has suffered from other damaging earthquakes in recent years, most notably the 1995 Kobe earthquake. This earthquake that shook the city of Kobe on January 17, 1995, measuring 7.2 magnitude, was the most devastating earthquake to strike Japan since the Kanto event in 1923. This earthquake occurred far from the known faults and was produced by an unknown fault, which was a strike-slip one. The strong shaken area stood on the alluvial deposits of the Rokko mountains in the north and the coastline in the south. Fig.5a shows the 2PRS recorded at JR Takatori station. One peak at 0.1 sec and another at 0.6 sec is clearly identified.

2.4 Gorkha, Nepal earthquake (2015)

The M 7.8 earthquake of April 25 struck central Nepal with its epicenter located in Gorkha district, about 80 km NW of Kathmandu. At the location of this earthquake, the India plate is converging with Eurasia at a rate of 45 mm/yr towards the north-northeast –a fraction of which (about 18 mm/yr) is driving the uplift of the Himalayan Mountain Range [10]. The Himalayan region is one of the most seismically active regions in the world producing significant seismic events. This event caused an unprecedented loss of life and devastation.

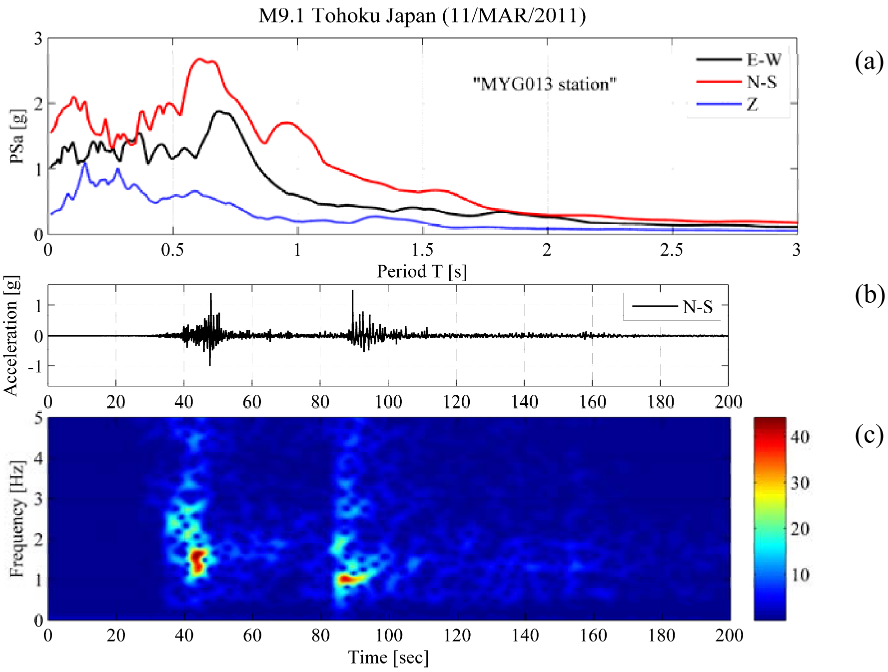

Fig. 4 – 2011 Japan earthquake recorded at MYG013 station: (a) 5%-damped acceleration response spectra (2PRS). (b) Acceleration time history for the N-S component. (c) Spectrogram for the N-S component.

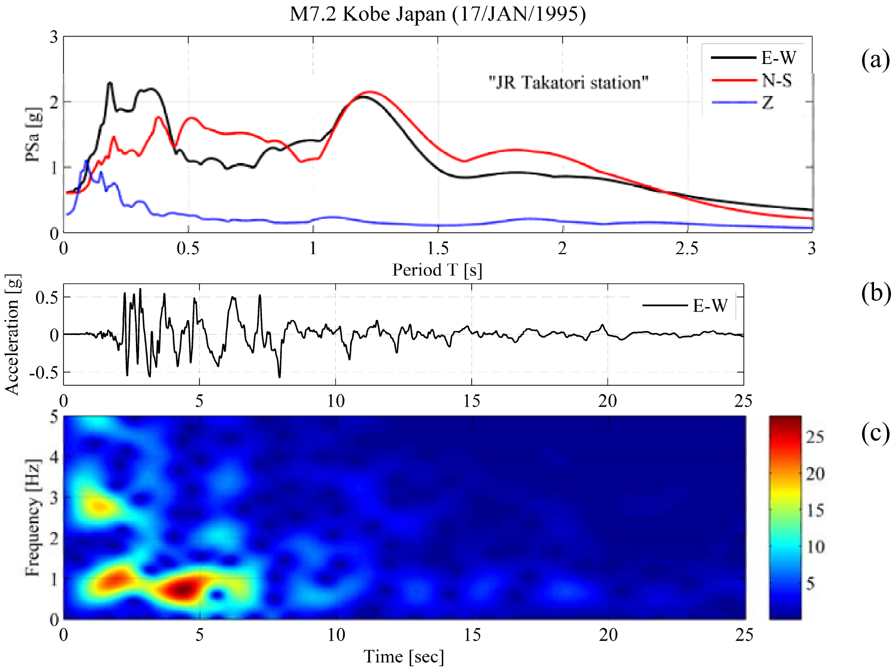

Fig. 5 – 1995 Japan earthquake recorded at JR Takatori station: (a) 5%-damped acceleration response spectra (2PRS). (b) Acceleration time history for N-S component. (c) Spectrogram for N-S component.

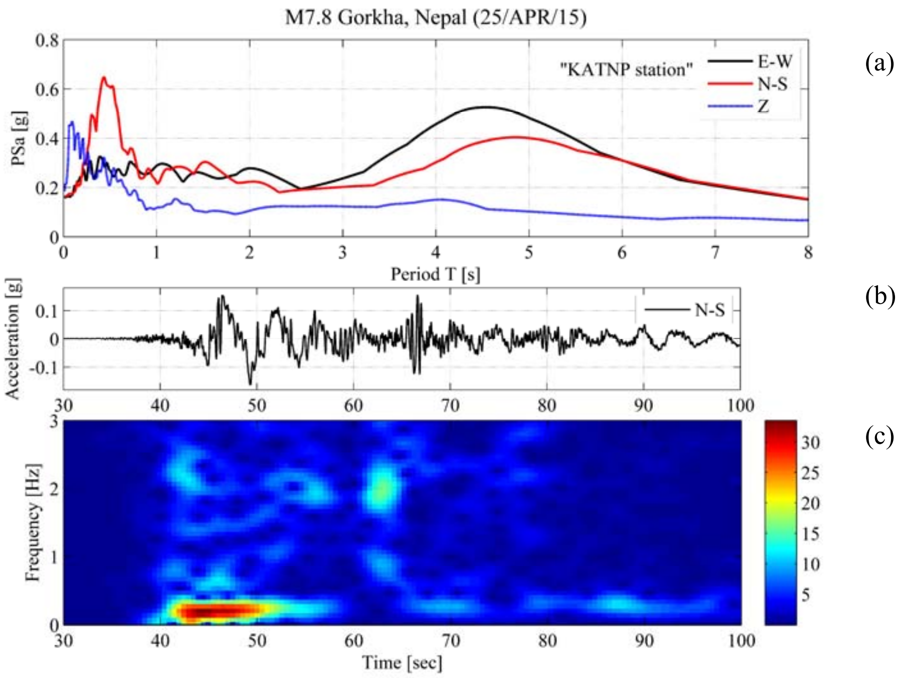

Fig. 6 – 2015 Nepal earthquake recorded at Kathmandu station: (a) 5%-damped acceleration response spectra (2PRS). (b) Acceleration time history for N-S component. (c) Spectrogram for N-S component.

The ground motions of this event were registered at USGS/CESMD station KATNP, Kathmandu. According to Fig.6a, response spectra of the recorded ground motions are presented. It is clear that in the short period range, the spectrum for the N-S component presents one peak around 0.5 seconds; while the second peak is evident between 4.0 and 6.0 seconds. The global Vs_{30} indicates that central part of Kathmandu valley has soft soil deposits that are typically NEHRP site class D (Vs_{30} between 180 and 360 m/s), and geologic studies show that thick semi-consolidated quaternary sediments cover the valley with the maximum depth of 550 m in its central part [14]. According to the period equation (Eq. (1)), the natural period would approach to 6 seconds (0.17 Hz), which could be due to the complex influence of underlying unconsolidated quaternary sediments in the basin. This period is in accordance with T = 6 seconds (0.17 Hz) identified in the spectrogram of Kathmandu station, N-S component (Fig.6c).

2.5 Muisne, Ecuador earthquake (2016)

The earthquake of April 16 was a powerful natural event, which occurred off the Ecuadorian Pacific coast. The M 7.8 earthquake occurred as the result of shallow thrust faulting generated at the gently sloping plate boundary fault that conveys the Nazca plate eastward and downward beneath the South America plate. The fault rupture, largely offshore, exceeded 60 km in width and extended nearly 160 km parallel to the coast [15]. Large damages and multiple building collapses in various cities (like Pedernales, Portoviejo, Manta, and Chone) were reported by reconnaissance teams [16].

This event is one of the few subduction zone earthquakes well registered in terms of the closeness of the accelerographic stations to the seismic source (36 km SW of the epicenter). Gallegos & Saragoni [17] performed a comprehensive analysis of the strong-motion accelerograms for 21 IG-EPN stations. The findings indicated higher values of peak ground acceleration (PGA), Arias Intensity (Ia), destructiveness potential factor (Pdh) and acceleration spectral ordinates (Sa) than those found for previous Chilean and Mexican earthquakes. These outcomes confirmed the observations indicating that Muisne earthquake was

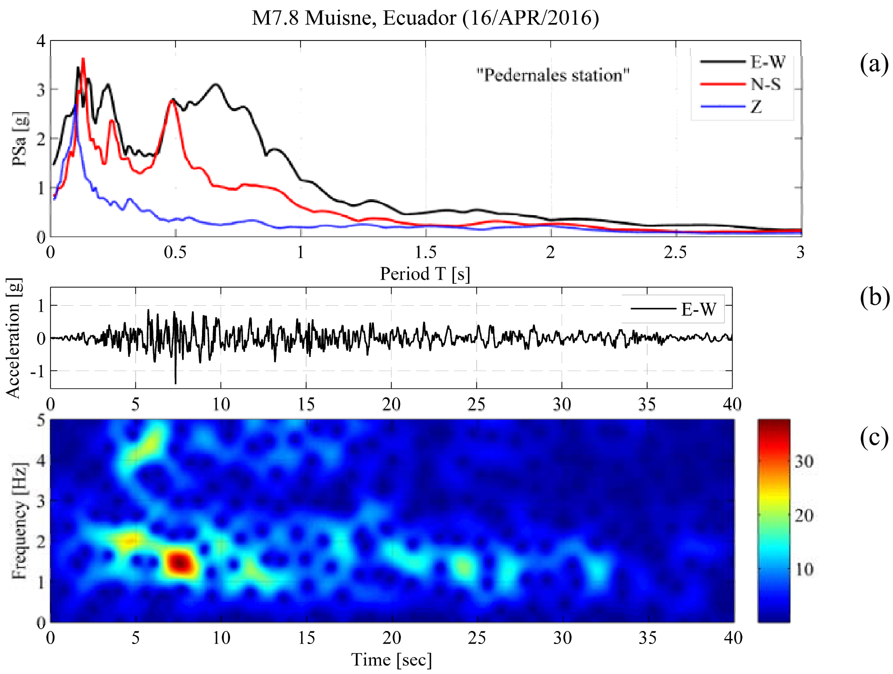

Fig. 7 – 2016 Ecuador earthquake recorded at Pedernales station: (a) 5%-damped acceleration response spectra (2PRS). (b) Acceleration time history for E-W component. (c) Spectrogram for E-W component.

destructive. Six stations presented accelerograms with destructive characteristics, which correspond to cities where damaging conditions and building collapses were largely observed.

Absolute acceleration response spectra, for 5% critical damping, for Pedernales station was computed (Fig.7a), which exhibit remarkable behavior. Pedernales (the nearest station to the epicenter) is characterized to have both horizontal spectra with two peaks. One of them around 0.2 sec, and another peak between 0.5 and 0.8 seconds. The spectrogram of the Fig.7c for the E-W component depicts energy pulses at periods of 0.5 sec (2.0 Hz) and 0.2 sec (4 Hz) in most of the acceleration time history. This feature is related to both the distance and site effect of soft soils that are typical of the coastal zone of Ecuador.

2.6 Norcia, Italy earthquake (2016)

The August 24 M 6.2 earthquake southeast of Norcia, Italy, occurred as the result of shallow normal faulting on a NW-SE oriented fault in the Central Apennines. This region is tectonically and geologically complex, involving both subduction of the Adria micro-plate beneath Eurasia and the Apennines from east to west, continental collision between the Eurasia and Nubia (Africa) plates building the Alpine mountain belt further to the north and the opening of the Tyrrhenian basin to the west (the latter of which is in turn related to Adria subduction and eastward trench migration). The August 24 normal faulting earthquake is an intraplate event, an expression of the east-west extensional tectonics that now dominate along the Apennine belt [18].

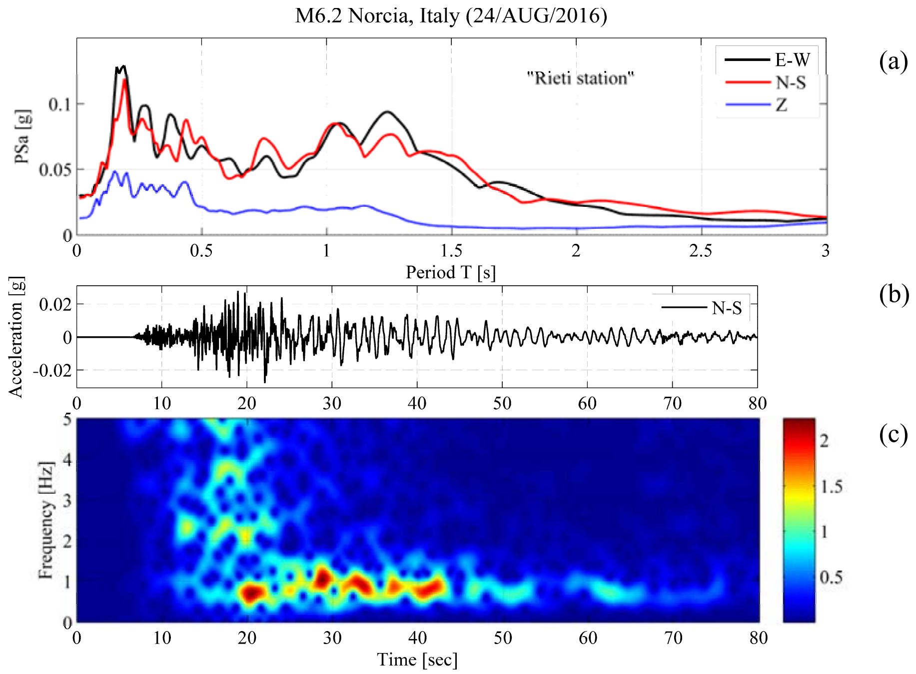

Fig. 8 – 2016 Italy earthquake recorded at Rieti station: (a) 5%-damped acceleration response spectra (2PRS). (b) Acceleration time history for E-W component. (c) Spectrogram for E-W component.

2.7 Puebla – Morelos, Mexico earthquake (2017)

September 19 M 7.1 earthquake in central Mexico occurred as the result of normal faulting at a depth of 48 km. The event is near, but not directly on, the plate boundary between the Cocos and North America plates in the region. The location, depth, and normal-faulting mechanism of this earthquake indicate that it is likely an intraplate event, within the subducting Cocos slab, rather than on the shallower megathrust plate boundary interface [19].

Ground motions of this event were registered at CIRES/RACM station Cibeles (CI05), Mexico City, located in the zone of soft soils (transition - lake edge) where buildings of 4~7 stories collapsed. Fig.9a illustrates absolute acceleration response spectra for 5% critical damping and shows the common 2PRS again, especially for the E-W component. The spectrum presents one peak around 0.4 sec and another peak between 1.6 and 1.7 seconds. Acceleration time history for this component is depicted in Fig.9b. Further, pulses of energy at 1.65 s (0.6 Hz) due to soil response and 0.4 s (2~3 Hz) due to the source are identified in the spectrogram (Fig.9c).

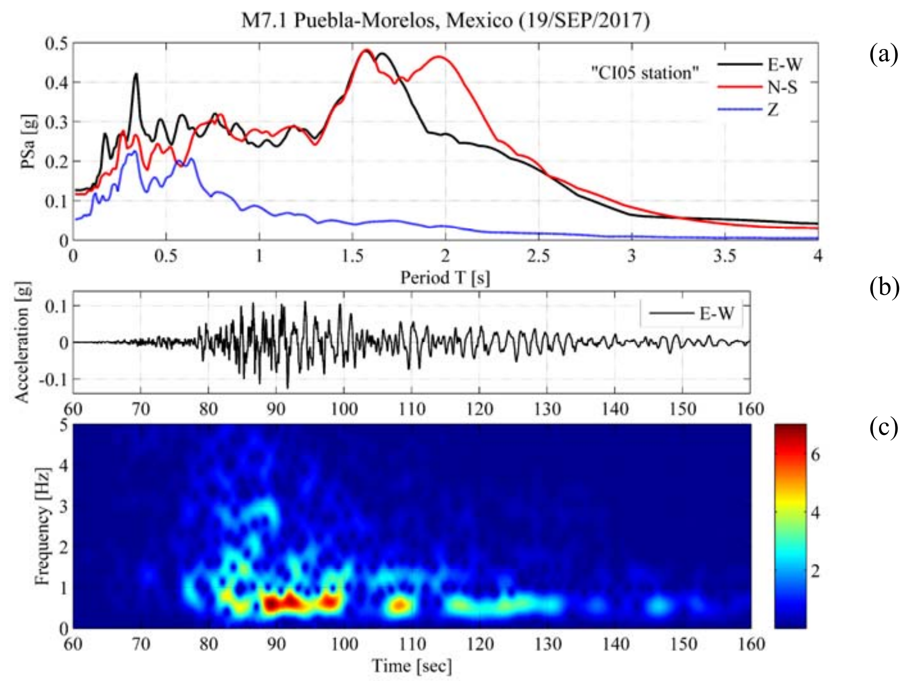

Fig. 9 – 2017 Mexico earthquake recorded at CI05 station: (a) 5%-damped acceleration response spectra (2PRS). (b) Acceleration time history for E-W component. (c) Spectrogram for E-W component.

3. Conclusions

Two-peak ground-motion response spectra (2PRS) have often been observed in epicentral or near-field accelerograms recorded in soft soils after the occurrence of subduction earthquakes during the last 35 years. Nevertheless, recent evidence depicts that this type of spectra could be also observed for earthquakes in other non-subduction zones. One of the peaks represents the highest energy content of the earthquake (short periods) while the other one the dynamic response of the soil (sites with long predominant period).

In this work, 2PRS corresponding to accelerograms registered in soft soils for latest subduction and non-subduction earthquakes are investigated. The studied seismic events produced significant building collapses and consequently losses of lives in the last decade: Chile, 2010; New Zealand, 2011; Japan, 2011; Nepal, 2015; Ecuador, 2016; Italy 2016; and Mexico, 2017. Usually, the soil peak is similar or larger amplitude than the source peak. However, for earthquakes related with short faults of a few kilometers, the amplitude of the soil peak never surpasses the first peak.

The actual importance of 2PRS for earthquake engineering and seismic design of structures (e.g., buildings) is that source peak affects houses or middle-rise buildings and soil peak affects high-rise or base-isolated buildings. Therefore, design response spectra considered in national seismic codes for soft soils should be modified in the future in order to consider both effects.

4. References

[1] Saragoni, G.R.; Ruiz S. Implication and New Challenges for the Seismic Design from the 2010 Chile Earthquake. Book: "M=8.8 Earthquake in Chile, February 27, 2010" (in Spanish). Santiago, Chile: University of Chile; 2012.

[2] Saragoni, G.R.; Gallegos MF. Evidence of two peaks response spectra (2PRS) due to separated effects of soil and source in recent subduction earthquakes. In: Silvestri & Moraci, editor. Earthq. Geotech. Eng. Prot. Dev. Environ. Constr., Rome, Italy: Associazione Geotecnica Italiana; 2019, p. 4848–56.

[3] Saragoni, G.R.; Gonzales, P.; Fresard M. Analysis of the Accelerograms of March 3, 1985, Chile Earthquake. Chapter 3. Book: "The March 3, 1985, Chile Earthquake". (in Spanish). Santiago, Chile: CAP; 1986.

[4] Lobos C. Effects of Source, Surface Waves and Soils in the Accelerograms of March 3, 1985, Chile Earthquake (in Spanish). University of Chile, 1999.

[5] Gómez BA. Interpretation of Soil Effects in Mexico Valley using the High-Density Accelerographic Network. (in Spanish). National Autonomous University of Mexico, 2002.

[6] Saragoni, G.R.; Ruiz S. Elastic Model 1D for the Soil Dynamic Response Obtained from the Analysis of Accelerograms of Chile Central Earthquake (in Spanish). 5th Chil. Congr. Geotech., Chile: 2004.

[7] Ruiz, S.; Saragoni GR. The proposition of 2 Peaks Acceleration Response Spectra for the Chilean Seismic Code Considering the Effects of Soil and the Type of Subduction Earthquake (in Spanish). IX Chil. Congr. Seismol. Earthq. Eng., Concepcion: 2005.

[8] Ruiz, S.; Saragoni GR. Two Peaks Response Spectra (2PRS) for Subduction Earthquakes Considering Soil and Source Effects. 14th World Conf. Earthq. Eng., China: 2008.

[9] Idini, B.; Rojas, F.; Ruiz, S.; Pasten C. Ground motion prediction equations for the Chilean subduction zone. Bull Earthq Eng 2017:1853–80.

[10] Hayes, G.P., Myers, E.K., Dewey, J.W., Briggs, R.W., Earle, P.S., Benz, H.M., Smoczyk, G.M. F, H.E., Barnhart, W.D., Gold, R.D., and Furlong KP. Tectonic summaries of magnitude 7 and greater earthquakes from 2000 to 2015. Virginia, USA: 2017.

[11] Ruiz, S.; Saragoni GR. Free vibration of soils during large earthquakes. Soil Dyn Earthq Eng 2009;29:1–16.

[12] Sandoval, M.; & Saragoni GR. Analysis of Seismic Demand in the Collapse of Alto Rio Building considering the propagation of waves during the earthquake of February 27, 2010 (in Spanish). XI Chil Congr Seismol Earthq Eng 2015.

[13] USGS. M 6.1 - South Island of New Zealand. (Last revised: February/2020) 2011. https://earthquake.usgs.gov/earthquakes/eventpage/usp000huvq/executive.

[14] Rai, D.C. Singhal, V. Raj, B. Sagar SL. Reconnaissance of the effects of the M7.8 Gorkha (Nepal) earthquake of April 25, 2015. Geomatics, Nat Hazards, Risk 2015.

[15] USGS. M 7.8 - 27km SSE of Muisne, Ecuador. (Last revised: February/2020) 2016. https://earthquake.usgs.gov/earthquakes/eventpage/us20005j32/executive.

[16] EERI. M 7.8 Muisne, Ecuador Earthquake on April 16, 2016. 2016.

[17] Gallegos, M.F.; Saragoni GR. Analysis of strong-motion accelerograph records of the 16 April 2016 Mw 7.8 Muisne, Ecuador earthquake. 16th World Conf. Earthq. Eng. 16WCEE, Santiago, Chile: 2017, p. 1–12.

[18] USGS. M 6.2 - 10km SE of Norcia, Italy 2016. https://earthquake.usgs.gov/earthquakes/eventpage/us10006g7d/executive.

[19] USGS. M 7.1 - 1km E of Ayutla, Mexico. (Last revised: February/2020) 2017. https://earthquake.usgs.gov/earthquakes/eventpage/us2000ar20/executive.

